Electronic band structure of SrCu$_4$As$_2$ and KCu$_4$As$_2$: Metals with diversely doped CuAs layers

V. G. Hadjiev,[1] Bing Lv,[2] and C. W. Chu[2,3]

[1]*Texas Center for Superconductivity and Department of Mechanical Engineering, University of Houston, Texas 77204-5002, USA*
[2]*Texas Center for Superconductivity and Department of Physics, University of Houston, Houston, Texas 77204-5002, USA*
[3]*Lawrence Berkeley National Laboratory, 1 Cyclotron Road, Berkeley, California 94720, USA*

We present a density functional study of SrCu$_4$As$_2$ and KCu$_4$As$_2$. The two isostructural compounds constitute a system that allows a broad range of doping of CuAs layers through nominally K$^+$ for Sr^{2+} substitution. SrCu$_4$As$_2$ (space group $R\bar{3}m$) is a metal having highly dispersive bands at E_F, two holelike Fermi sheets in the form of corrugated cylinders along Γ-Z and electron pockets around F points in the rhombohedral Brillouin zone. Cu 3d states are located at 2.5 eV below E_F, giving little contribution to the bands near E_F. The F-point electron pockets disappear in KCu$_4$As$_2$ and the compound exhibits a large multisheet two-dimensional Fermi surface with a somewhat enhanced d character through Cu 3d-As 4p bonding. Despite shifting E_F toward the Cu 3d bands in KCu$_4$As$_2$, the compound remains with completely populated d shells and it is unlikely to exhibit superconductivity of a type similar to that in the ternary iron arsenides.

The discovery of layered FeAs-based high-temperature superconductors[1–5] has sparked an extensive quest for different superconductors with closely related structures but containing other transition metals (Tm) and/or pnictogens (Pn). This approach, however, to the best of our knowledge, so far has not yielded any TmPn superconductors with T_c as high as and superconductivity type as close to those of the FeAs superconductors.[6] One of the most prominent substitutional doping in FeAs compounds is that of Tm for Fe. The substitution of nominal Fe^{2+} (3d^6) in the double-layered, "122," AFe$_{2-x}$Tm$_x$As$_2$ (A = Ba, Sr) with Tm = Co^{2+} (3d^7) and Ni^{2+} (3d^8) results in superconducting compositions for x = 0.12–0.20 (Ref. 6) and x = 0.06–0.23,[7] respectively, due to electron doping in the Fe 3d band. Doping with Mn^{2+} (3d^5) and Cr^{2+} (3d^4) yields only nonsuperconducting mixed compounds.[6] On the other hand, complete substitution of As with P results at best in conventional-like superconductors with modest, liquid-helium (LH) range, T_c.

Virtually all known FeAs superconductors have been studied using the density functional theory (DFT). The characteristic electron band structure of FeAs superconductors features a Fermi surface dominated by Fe 3d bands broaden by metal-metal d bonding, nearly anionic As, and weak As-As interactions.[8,9] Within the 122 system, CoAs- and NiAs-based compounds have an electronic band structure similar to that of parent FeAs compounds. These findings, along with the higher number of 3d electrons, are likely the reasons for Co and Ni doping of parent FeAs-122 to produce superconducting mixed compositions. In TmAs-122 compounds with Tm = Mn and Cr, the strong spin-dependent hybridization between Mn(Cr) 3d and As 4p states drives the compounds to antiferromagnetic semiconducting (MnAs-122) (Ref. 10) or metallic (CrAs-122) (Ref. 11) states. Doping of FeAs-122 with Mn and Cr with a lower number of 3d electrons than that of Fe leaves the mixed compounds nonsuperconducting.

Divalent copper, Cu^{2+}, is a transition-metal ion with a 3d^9 shell configuration and therefore it is a potential direct d-band dopant for FeAs-122 compounds. The electronic band structure of BaCu$_2$As$_2$ and SrCu$_2$As$_2$,[12] however, is much

different than that of FeAs-122 and suggests that Cu is an ineffective dopant toward inducing superconductivity in FeAs-122. Indeed, the Cu 3d bands in CuAs-122 are located at 3 eV below E_F, the Cu d shell is fully occupied and gives little contribution to E_F, and CuAs-122 are sp-band metals.[12] Nevertheless, we believe that further DFT studies of the CuAs system will shed more light on the bonding in the CuAs system, particularly in view of the existence of closely related to CuAs-122 but more complex KCu$_4$As$_2$ (Ref. 13) and SrCu$_4$As$_2$ (Ref. 14) compounds.

In this Brief Report we present the results of DFT calculations of "142" compounds, SrCu$_4$As$_2$ and KCu$_4$As$_2$. The CuAs-142 structure allows a broad range of doping by substitution of nominally Sr^{2+} with K$^+$. We show that the difference in the electronic structures of the two compounds is not merely a doping effect, that is, changing E_F, but also involves a rearrangement of electronic bands close to E_F.

The first-principles calculations were done within the generalized-gradient approximation (GGA) with the Perdew-Burke-Ernzerhof (PBE) exchange-correlation functional[15] using the norm-conserved pseudopotential plane-wave method as implemented in the CASTEP code.[16] The electronic band structure, related properties, and geometry optimization of the structures were calculated self-consistently (SCF) with a 880-eV kinetic energy cutoff for the plane waves and a SFC tolerance better than 5×10^{-7} eV/atom over $24 \times 24 \times 24$ Monkhorst-Pack grid in the k space. The compounds were treated as metallic systems and partial electron occupancy was allowed during the SCF energy minimization to eliminate discontinuous changes in total energy when a band crosses E_F. Gaussian smearing with a smearing width of 0.026 eV was applied during electronic minimization to each energy level to simulate an electronic temperature close to room temperature.

SrCu$_4$As$_2$ and KCu$_4$As$_2$ crystallize in a structure described by the space group $R\bar{3}m$ (No. 166).[13,14] The unit cell of the ACu$_4$As$_2$ (A = Sr, K) crystal structure is shown in Fig. 1(a) in a hexagonal axes' presentation and in (b) as a primitive rhombohedral cell. The lattice constants, internal parameters,
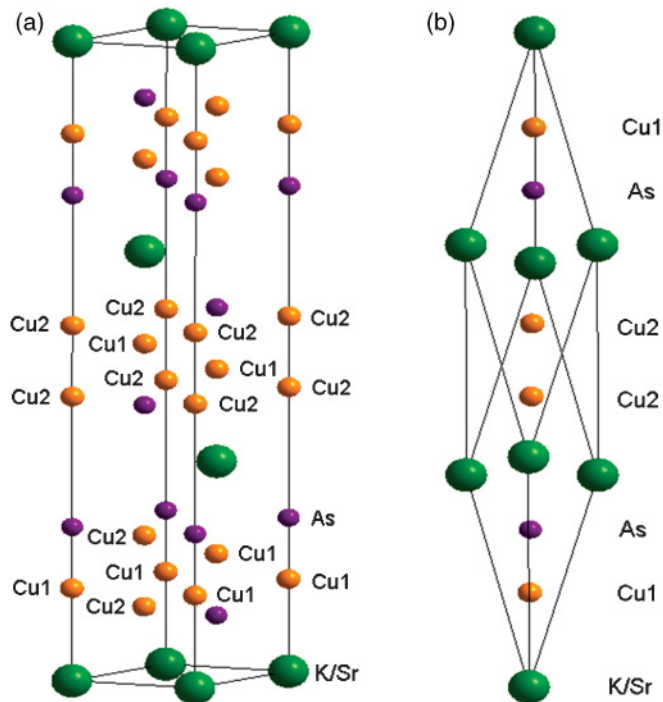
FIG. 1. (Color online) Crystal structure of K/SrCu$_4$As$_2$ presented in hexagonal axes (a) and its primitive rhombohedral cell (b) containing one formula unit.

and selected interatomic distances of SrCu$_4$As$_2$ and KCu$_4$As$_2$ used in the electronic band-structure calculations are listed in Table I. We preserved the value of the experimental lattice constants during optimization of the structures through relaxing only the z-internal parameters within the Broyden-Fletcher-Goldfarb-Shannon (BFGS) minimization scheme.[17] The parameters for all structures in Table I were determined after the minimization convergence tolerances were satisfied:

TABLE I. Crystal structure parameters for KCu$_4$As$_2$ and SrCu$_4$As$_2$, space group $R\bar{3}m$ (No. 166). a,c and a_{rh},γ are the lattice parameters in hexagonal and rhombohedral cell presentations, respectively. The asterisk denotes interatomic distances along the c axis, that is, those seen also in the simpler rhombohedral cell. The crystal structures were optimized with relaxed z-internal parameters and using the experimental lattice constants reported in Refs. 13,14.

Parameters	KCu$_4$As$_2$	SrCu$_4$As$_2$
a (Å)	4.120 (Ref. 13)	4.203 (Ref. 14)
c (Å)	25.956 (Ref. 13)	23.452 (Ref. 14)
a_{rh} (Å)	8.973	8.185
γ (deg)	26.54	29.75
z_{As}	0.2422	0.2496
z_{Cu1}	0.1448	0.1440
z_{Cu2}	0.4414	0.4370
d^*_{Cu1-As} (Å)	2.528	2.477
d_{Cu1-As} (Å)	2.759	2.808
d_{Cu2-As} (Å)	2.419	2.471
d^*_{Cu2-As} (Å)	5.170	4.395
$d^*_{Cu2-Cu2}$ (Å)	3.043	2.954
$d^*_{K/Sr-Cu1}$ (Å)	3.758	3.377

5×10^{-6} eV/atom for energy, 0.01 eV/Å for forces, 0.02 GPa for stresses, and 5×10^{-4} Å for displacements. The crystal structure of CuAs-142 is more complicated than that of CuAs-122. Although it retains the CuAs-layered structure, Cu occupies two inequivalent positions and both Cu and As are characterized by z internal parameters.

Figure 2 shows the calculated electron density of states (DOS) per formula unit (f.u.) of SrCu$_4$As$_2$ and KCu$_4$As$_2$. The partial DOS of SrCu$_4$As$_2$ reveals high binding energy Cu $3d$ bands located at more than 2.5 eV below E_F. The Cu $3d$ band contribution at E_F is small, 0.18 eV^{-1}/f.u., and the Fermi surface is dominated by p-state bands, that is, Sr-142 is more a p-band type of metal rather than an sp-band one as Sr-122.[9] The effect of Sr substitution with the lower number of valence electrons K is most notably seen in decreasing Cu $3d$ binding energy by 0.5 eV; the Cu $3d$ band contribution at E_F increases to 0.54 eV^{-1}/f.u. (0.135 eV^{-1}/Cu) but it is still an order of magnitude lower than 1.53–2.62 eV^{-1}/Fe in FeAs compounds.[18] The inset in Fig. 2 (lower panel) indicates a hybridization between d and p states close to E_F and KCu$_4$As$_2$ can be classified as a pd-band metal. The DOS of Cu $3d$ bands in both compounds exhibits two sharp peaks that correspond to the $3d$ states of the two inequivalent Cu atoms. The crystal-field
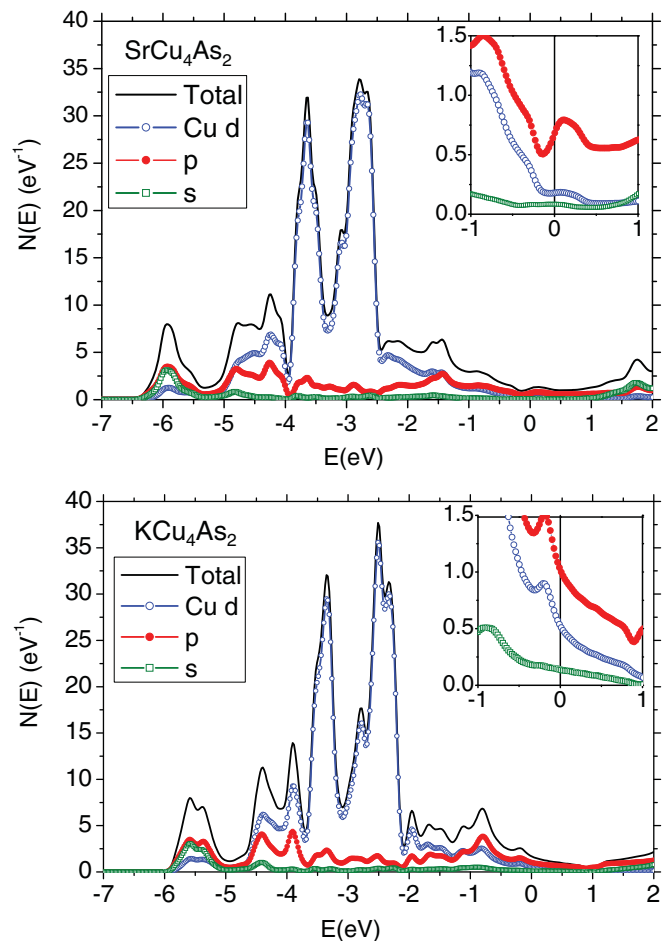

FIG. 2. (Color online) Electron density of states (DOS) of SrCu$_4$As$_2$ (top) and KCu$_4$As$_2$ (bottom) calculated per formula unit (content of a primitive cell). The insets present a closeup of the partial DOS near the Fermi energy $E_F = 0$.

symmetry at Cu sites in CuAs-142 is trigonal, C_{3v}, and one expects a split of the d states into a triplet comprising d_{z^2}, (d_{xy}, $d_{x^2-y^2}$), and (d_{xz}, d_{yz}) states. The dominating double-peak structure in the d-band DOS shown in Fig. 2 indicates a very weak splitting that, along with d-band broadening due to d-d interaction, results in overlapping of the split components. We note, however, that part of the Cu $3d$ states hybridize with the As $4p$ states and produce ($p + d$)-band DOS wings at the lower (-4 to -5 eV) and the higher (-2.5 eV to E_F) sides of the double Cu $3d$ peak. Lowering of E_F with K for Sr substitution places E_F in KCu$_4$As$_2$ at an increased ($p + d$) DOS as seen in the inset of Fig. 2(b) .

The spin-polarized band-structure calculations (not presented here) give negligibly small magnetic moments for the two compounds. This result corroborates with the low value of nonpolarized $3d$ DOS at $N(E_F)$, in both compounds, which also indicates that the compounds are away from any instability toward ferromagnetism. According to the Stoner criterion, a compound is unstable toward itinerant ferromagnetism provided $N(E_F)I_S > 1$, where for Cu ions the parameter I_S is 0.5–0.7 eV.[19] This criterion is apparently not satisfied in SrCu$_4$As$_2$ and KCu$_4$As$_2$

Next we note that in Fig. 2 the density of states of SrCu$_4$As$_2$ and KCu$_4$As$_2$ has a local maximum at 0.12 eV above and 0.21 eV below E_F, respectively. The origin of these DOS peaks is seen in Fig. 3, which displays the calculated band structure along directions connecting the high symmetry points in the Brillouin zone. Three bands cross E_F in the band structure of SrCu$_4$As$_2$, as shown in Fig. 3(a). Two are holelike, As $4p_x$ and $4p_y$, bands with weak dispersion along Γ-Z that contributes to the DOS peak at 0.12 eV above E_F (Fig. 2, upper panel). The third one is an As $4p_z$ electronic band with the bottom at the F point, that is, SrCu$_4$As$_2$ is a partially compensated metal with properties more typical for semimetals than for metals. A second pair of As $4p_x$ and $4p_y$ bands with a similar dispersion is completely populated and lies at 0.25 eV below E_F. Cu1 and Cu2 form two different trigonal surroundings of As in the xy plane perpendicular to the hexagonal axis. As a result, the two pairs of $4p_x$ and $4p_y$ bands are shifted in energy.

The band structure of KCu$_4$As$_2$ shown in Fig. 3(b) resembles that of SrCu$_4$As$_2$ but with some notable differences. Apart from the hole-doping effect, which lowers E_F with respect to the main body of electronic bands, the band at the F point shifts above E_F simultaneously with the top of the second pair of $4p_x$ and $4p_y$ bands, the latter due mainly to band broadening. This way four, predominantly hole-type, bands cross E_F in the band structure KCu$_4$As$_2$, as shown in Fig. 3(b).

The Fermi surfaces (FSs) of SrCu$_4$As$_2$ and KCu$_4$As$_2$ are shown in Figs. 4(a) and 4(b), respectively. SrCu$_4$As$_2$ is a three-dimensional (3D) metal, however, its holelike FS has
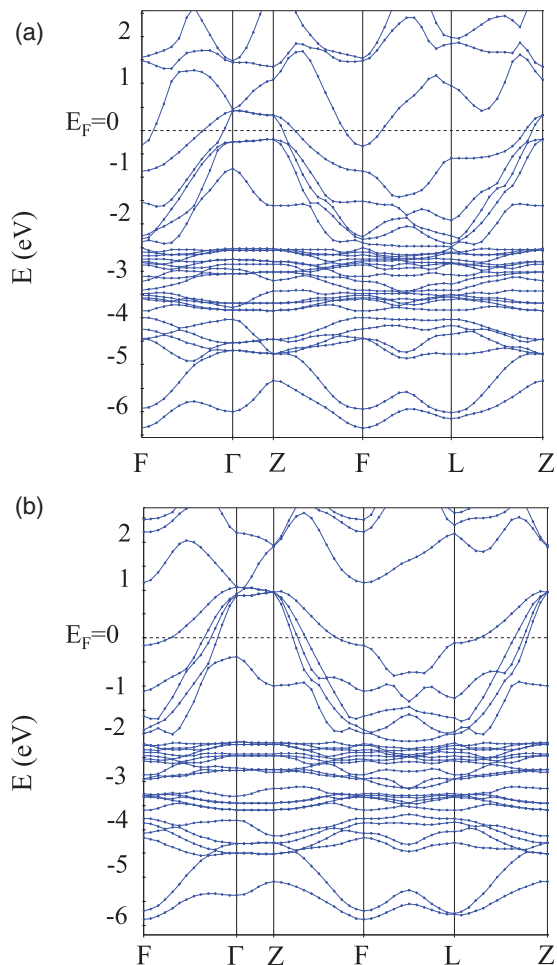

FIG. 3. (Color online) Calculated band structure of SrCu$_4$As$_2$ (a) and KCu$_4$As$_2$ (b) using the experimental lattice parameters and optimized internal coordinates.
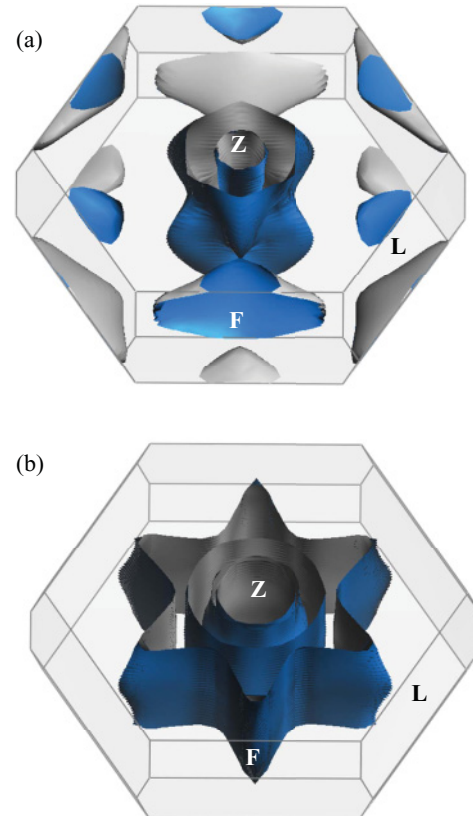

FIG. 4. (Color online) Fermi surface of SrCu$_4$As$_2$ (a) and KCu$_4$As$_2$ (b) plotted in the Brillouin zone of the rhombohedral primitive cell.

more of a two-dimensional (2D) character and appears as a corrugated cylinder with an axis along Γ-Z. This particular FS develops further into a six-pointed star shape in KCu_4As_2. The points are related to the van Hove singularity in the band dispersion around the F and L points in the Brillouin zone [Fig. 3(b)], resulting also in the DOS peak at 0.21 eV below E_F. The FS of KCu_4As_2 reveals a more 2D metallic character than that of $SrCu_4As_2$. The average Fermi velocity along the c axis in KCu_4As_2, $\langle v_c^2 \rangle^{1/2}$, is 0.42×10^6 m/s and in the ab plane, normal to the c axis, $\langle v_{ab}^2 \rangle^{1/2} = 1.90 \times 10^6$ m/s. The corresponding Fermi velocity anisotropy in $SrCu_4As_2$ is smaller: $\langle v_c^2 \rangle^{1/2} = 0.58 \times 10^6$ m/s and $\langle v_{ab}^2 \rangle^{1/2} = 1.11 \times 10^6$ m/s for the holelike component and $\langle v_c^2 \rangle^{1/2} = 1.10 \times 10^6$ m/s and $\langle v_{ab}^2 \rangle^{1/2} = 1.55 \times 10^6$ m/s for the electronic band. Since the holelike and electron charge carriers in $SrCu_4As_2$ are partially compensated, the dominant-type carriers determined by the transport measurements may change with temperature, as it is been reported recently,[20] depending on the relative concentration of the two types of carriers and scattering mechanisms.

In conclusion, the DFT calculations of $SrCu_4As_2$ and KCu_4As_2 show that K for Sr substitution has a profound doping effect that turns the compensated, close to semimetal, Sr-142 into a large Fermi surface K-142 metal while preserving the crystal structure. In both compounds the Cu $3d$ bands are completely populated, chemically inert, which makes it unlikely for $SrCu_4As_2$ and KCu_4As_2 to develop a type of superconductivity at low temperatures that is similar to that in ternary iron arsenide superconductors.

[1]Y. Kamihara, T. Watanabe, M. Hirano, and H. Hosono, J. Am. Chem. Soc. **130**, 3296 (2008).

[2]M. Rotter, M. Tegel, and D. Johrendt, Phys. Rev. Lett. **101**, 107006 (2008).

[3]K. Sasmal, B. Lv, B. Lorenz, A. M. Guloy, F. Chen, Y. Y. Xue, and C. W. Chu, Phys. Rev. Lett. **101**, 107007 (2008).

[4]X. C. Wang, Q. Q. Liu, Y. X. Lv, W. B. Gao, L. X. Yang, R. C. Yu, F. Y. Li, and C. Q. Jin, Solid State Commun. **148**, 538 (2008).

[5]J. H. Tapp, Z. J. Tang, B. Lv, K. Sasmal, B. Lorenz, P. C. W. Chu, and A. M. Guloy, Phys. Rev. B **78**, 060505 (2008).

[6]D. C. Johnston, Adv. Phys. **59**, 803 (2010).

[7]L. J. Li, Y. K. Luo, Q. B. Wang, H. Chen, Z. Ren, Q. Tao, Y. K. Li, X. Lin, M. He, Z. W. Zhu, G. H. Cao, and Z. A. Xu, New J. Phys. **11**, 025008 (2009).

[8]D. J. Singh and M.-H. Du, Phys. Rev. Lett. **100**, 237003 (2008).

[9]D. J. Singh, Phys. Rev. B **78**, 094511 (2008).

[10]J. An, A. S. Sefat, D. J. Singh, and M. H. Du, Phys. Rev. B **79**, 075120 (2009).

[11]D. J. Singh, A. S. Sefat, M. A. McGuire, B. C. Sales, D. Mandrus, L. H. VanBebber, and V. Keppens, Phys. Rev. B **79**, 094429 (2009).

[12]D. J. Singh, Phys. Rev. B **79**, 153102 (2009).

[13]W. Weise and H.-U. Schuster, Z. Anorg. Allg. Chem. **535**, 143 (1986).

[14]J. Dünner and A. Mewis, Z. Anorg. Allg. Chem. **625**, 625 (1999).

[15]J. P. Perdew, K. Burke, and M. Ernzerhof, Phys. Rev. Lett. **77**, 3865 (1996).

[16]S. J. Clark, M. D. Segal, C. J. Packard, P. J. Hasnip, M. I. J. Probert, K. Refson, and M. C. Payne, Z. Kristallogr. **220**, 567 (2005).

[17]B. G. Pfrommer, M. Cote, S. G. Louie, and M. L. Cohen, J. Comput. Phys. **131**, 133 (1997).

[18]D. J. Singh, Phys. Rev. B **78**, 094511 (2008).

[19]L. Ortenzi, S. Biermann, O. K. Andersen, I. I. Mazin, and L. Boeri, Phys. Rev. B **83**, 100505 (2011).

[20]B. Lv, B. Lorenz, M. Gooch, F. Chen, L. Deng, and C. W. Chu [http://meetings.aps.org/link/BAPS.2011.MAR.D23.1] (2011).